

AQ1 1 Analytical study of growth estimates, control of fluctuations, 2 and conservative structures in a two-field model of the scrape-off layer

3 R. Vilela Mendes^{a)} and João P. S. Bizarro^{b)}

4 *Instituto de Plasmas e Fusão Nuclear, Instituto Superior Técnico, Universidade de Lisboa, 1049-001 Lisboa,*
5 *Portugal*

6 (Received 1 August 2016; accepted 9 December 2016; published online xx xx xxxx)

7 Anomalous transport, turbulence, and generation of large-scale, collective structures (so-called
8 blobs) in the scrape-off layer (SOL) of tokamaks are some of the main issues that control the
9 machine performance and the life expectancy of plasma-facing components, and here one tries to
10 achieve some understanding of these questions through a theoretical, analytical study of a reduced
11 two-dimensional two-field (density plus vorticity) model of the SOL. The model is built around a
12 conservative system describing transport perpendicular to the magnetic field in a slab geometry, to
13 which terms are added to account for diffusion and parallel losses (both for particles and current)
14 and to mimic plasma flow from the core (in the form of a source). Nonlinear estimates for the
15 growth rates are derived, which show the growth in the density gradient to be bounded above by
16 the vorticity gradient, and vice-versa, therefore suggesting a nonlinear instability in the model.
17 The possibility of controlling fluctuations by means of a biasing potential is confirmed (negative
18 polarisations being shown to be more effective in doing so, thus providing an explanation for what
19 is seen in experiments), as well as the advantage in reducing the inhomogeneity of the magnetic
20 field in the SOL to decrease the plasma turbulence there. In addition, focusing on the conservative
21 part of the equations, exact solutions in the form of travelling waves are obtained which might be
22 the conservative ancestors of the blobs that are observed in experiments and in numerical simula-
23 tions. [<http://dx.doi.org/10.1063/1.4973222>]

24 I. INTRODUCTION

25 Transport in the plasma boundary is one of the main pending
26 issues pertaining to the design and operation of future
27 fusion machines, the physics of particle and energy flows in
28 the boundary impacting both on machine performance and on
29 the life expectancy of plasma-facing components.¹⁻⁴ The
30 modelling of this plasma boundary, or scrape-off layer (SOL),
31 being extremely complex,⁵⁻¹¹ numerical codes have been
32 developed with recourse to reduced two-field models and con-
33 servation laws, greatly simplifying the analysis of the SOL
34 transport while retaining the fundamental properties of the
35 underlying physics, which is that of plasma turbulence.¹²⁻¹⁸
36 The broad picture coming out from these efforts is that,
37 although small-scale turbulence dominates, there may also be
38 large-scale coherent structures, associated with intermittent
39 events known as blobs, that are observed both in experiments
40 and in numerical simulations and greatly contribute to the
41 nature of particle and energy transport.^{2,4,6,9-11,14-16,19-22}
42 These blobs, besides modifying the local transport properties
43 through nonlinear interaction with small-scale turbulence, gen-
44 erate machine-scale flows that may seriously damage the wall
45 due to thermal charge asymmetries and plasma ejection.

46 In this article, one will try to achieve some understand-
47 ing on these questions through the analytical study of a
48 reduced two-dimensional (2D) fluid model, describing the
49 plasma dynamics (electrons plus current) perpendicular to
50 the magnetic field, built from a conservative model²³ (itself a

51 cold-ion, reduced version of more complete four-field mod- 51
52 els^{24,25}) to which phenomenological terms are added 52
53 accounting for particle and current diffusion, parallel losses, 53
54 and a core-plasma source.¹³⁻¹⁸ Emphasis will be on some 54
55 mathematical properties of the model, more precisely, on 55
56 obtaining nonlinear growth estimates for the physical quanti- 56
57 ties and on discussing the eventual control of fluctuations, 57
58 not only by polarization^{14,17,18,26,27} but also by acting on the 58
59 magnetic inhomogeneity. In addition, and focusing on the 59
60 conservative part of the equations, one aims at deriving exact 60
61 solutions that might be the conservative ancestors of the col- 61
62 lective structures related with blobs. In fact, one will revisit 62
63 in this paper, but in a purely analytical approach, a model 63
64 that is fairly standard in SOL turbulence,¹³⁻¹⁸ so that one 64
65 will not only recover some results already known from linear 65
66 stability analysis of interchange turbulence in the SOL (such 66
67 as the destabilising role of a negative density gradient and 67
68 the stabilising effects of the vorticity gradient and of a 68
69 reduced magnetic-field inhomogeneity^{14,15}), but will also 69
70 derive other results that are indeed new. These include the 70
71 setting up of upper bounds on the nonlinear growth rates for 71
72 the gradients of the density and electrostatic potential, the 72
73 unveiling of the benefits in using negative instead of positive 73
74 biasing when looking for improved stability (in agreement 74
75 with experimental results^{26,27}), and the obtention of exact 75
76 solutions of the traveling-wave type to the conservative ker- 76
77 nel around which the model is built. 77

78 It should be stressed that one of the motivations for the 78
79 present article was to push as far as possible the analytical 79
80 exploration of a model frequently used in studies of SOL tur- 80
81 bulence,¹³⁻¹⁸ an approach that is rarely followed in the field 81

^{a)}Also at Centro de Matemática e Aplicações Fundamentais, Universidade
de Lisboa. Electronic mail: rvilela.mendes@gmail.com

^{b)}Electronic mail: bizarro@ipfn.tecnico.ulisboa.pt

82 given the extreme complexity of SOL physics. Moreover, 133
 83 faced with model equations one suspects describe unstable 134
 84 behavior, it is essential to have some analytic control over 135
 85 their solutions, otherwise it might be hard to unravel what is 136
 86 a physically relevant behavior from what is a result of 137
 87 numerical instability when running simulation codes. 138
 88 Whenever necessary, simplifications will be made, yet 139
 89 always keeping in mind the aphorism according to which 140
 90 “everything should be made as simple as possible, but not 141
 91 simpler.” This is why, for instance, one chose to work in the 142
 92 limit of negligible ion temperature, and thus started from the 143
 93 cold-ion limit of a conservative two-field model for the den- 144
 94 sity and vorticity,²³ to end up with a model which, albeit 145
 95 simpler for not containing finite-ion-temperature effects, still 146
 96 retains the essential features of turbulent transport in the 147
 97 SOL.^{13–18} 148

98 So, this paper is structured as follows: the model is pre- 149
 99 sented and discussed in Sec. II, some estimates on nonlinear 150
 100 growth rates are offered in Sec. III, the control of turbulent 151
 101 fluctuations is dealt with in Sec. IV, the link between coher- 152
 102 ent structures and conservative dynamics is examined in Sec. 153
 103 V, and, finally, the findings and conclusions are summarized 154
 104 in Sec. VI. This outline corresponds to the story told below 155
 105 using an analytical language: after recognizing (from esti- 156
 106 mates of the global growth rates) that the model may exhibit 157
 107 a nonlinear unstable behavior, the control of unstable modes 158
 108 in the fluctuation spectrum (while still in the linear regime) 159
 109 is addressed, before showing how solutions of the conserva- 160
 110 tive part of the model can lead to large propagating struc- 161
 111 tures (that very much look like ejected blobs). Also, for 162
 112 completeness and while avoiding to burden the main text, 163
 113 mathematics that is eminently calculatory and straightfor- 164
 114 ward, but may be helpful when going through the details of 165
 115 the derivations, is provided in an Appendix through a series 166
 116 of notes.

117 II. THE MODEL

118 The starting point is the two-field (density plus vorticity) 157
 119 model 158

$$\frac{\partial Ln}{\partial t} = -[\phi, Ln] - \left[\phi, \frac{1}{B} \right] + \left[Ln, \frac{1}{B} \right] \quad (1a)$$

$$\frac{\partial \nabla^2 \phi}{\partial t} = -[\phi, \nabla^2 \phi] + \left[Ln, \frac{1}{B} \right] \quad (1b)$$

120 describing the dynamics perpendicular to the magnetic field, 158
 121 which can be extracted from a four-field model including 159
 122 finite-Larmor-radius effects, drift-velocity ordering, and 160
 123 gyroviscous terms,²⁴ provided the dynamics along the mag- 161
 124 netic field (the so-called parallel dynamics) is suppressed, 162
 125 the poloidal magnetic fluctuations are neglected, and the 163
 126 cold-ion limit is taken.²³ Hereabove, $Ln(x_1, x_2, t)$ stands for 164
 127 the log-density, meaning the logarithm of the normalised 165
 128 density $n(x_1, x_2, t)$, $\phi(x_1, x_2, t)$ for the normalised electro- 166
 129 static potential, and $B(x_1)$ for the normalised ambient 167
 130 magnetic field, $x_1 = (r - a)$ and $x_2 = a\theta$ are the radial 168
 131 poloidal coordinates, respectively, with a the minor radius of 169
 132 the core plasma (space being rescaled by the ion sonic 170

Larmor radius and time by the ion cyclotron frequency), the 133
 canonical Poisson bracket $[f, h]$ is given by $[f, h] = \partial_1 f \partial_2 h$ 134
 $-\partial_2 f \partial_1 h$, and the del operator reads $\nabla = (\partial_1, \partial_2)$, with ∂_i 135
 $= \partial/\partial x_i$. The conservative model in (1) has a simple 136
 Hamiltonian structure, which would be lost if finite ion- 137
 temperature effects (in particular, ion gyroviscosity) were 138
 retained in Equation (1b) for $\nabla^2 \phi$ while keeping compress- 139
 ibility (conveyed by the $1/B$ terms) in the continuity equation 140
 (1a), the manufacturing of a Hamiltonian form in such a case 141
 having been addressed by means of a so-called gyromap.^{23,25} 142
 To expect a reduced model to keep the Hamiltonian structure 143
 of the distant parent (Maxwell–Vlasov) model seems too 144
 stringent a requirement, one that might collide with the physi- 145
 cal interpretation and the simplicity of reduced models, inas- 146
 much as Hamiltonian systems are, in fact, just a small class 147
 among the conservative systems (in the Liouville sense).²⁸ 148

To this conservative model, and as described in the liter- 149
 ature,^{13–18} one adds diffusion (to govern the damping at small 150
 scales via the coefficients D and ν , respectively, for particles 151
 and vorticity), sinks (to mimic the parallel losses to the wall 152
 or limiter as set, from sheath physics,^{1,12} by the floating 153
 potential Λ and some $\sigma_{||}$ that measures the characteristic time 154
 for parallel transport), and a source $S(x_1)$ (to account for the 155
 plasma flow from the core). Hence, and putting 156

$$\tilde{g} = g = \partial_1 \left(\frac{1}{B} \right), \quad (2)$$

(1) is completed to become [see (a) in the Appendix] 157

$$\frac{\partial Ln}{\partial t} = -[\phi, Ln] - \tilde{g} \partial_2 (Ln - \phi) + D(\nabla^2 Ln + |\nabla Ln|^2) - \sigma_{||} e^{(\Lambda - \phi)} + S \quad (3a)$$

$$\frac{\partial \nabla^2 \phi}{\partial t} = -[\phi, \nabla^2 \phi] - g \partial_2 Ln + \nu \nabla^4 \phi + \sigma_{||} [1 - e^{(\Lambda - \phi)}], \quad (3b)$$

which account for particle balance (for electrons) and charge 158
 conservation, respectively. It is worth mentioning that (3) is 159
 very much the same as a 2D model used for flux-driven uni- 160
 form-temperature (so-called FDUT) simulations,^{15,16} and 161
 also very similar to TOKAM-2D,^{12–14,17,18} the difference 162
 with the latter lying in the presence hereabove of the term 163
 associated with the magnetic field inhomogeneity \tilde{g} in the 164
 continuity equation, so all results in this paper apply to 165
 TOKAM-2D by making $\tilde{g} = 0$. The compressibility term in 166
 (3a), namely, $\tilde{g} \partial_2 (Ln - \phi)$, being of the same order as the 167
 coupling term $g \partial_2 Ln$ in the vorticity equation, one has 168
 decided to keep it in the model, as other authors have 169
 done.^{6,8,9,15,16} For completeness, note that interchange-like 170
 models similar to the one above have also been used to study 171
 the nonlinear dynamics of transport-barrier relaxations and 172
 of tearing magnetic islands.^{29–31} 173

174 III. NONLINEAR GROWTH ESTIMATES

To estimate the dependence of the temporal growth rate 175
 of physical quantities, (3) will be simplified: first, one will 176
 assume that the difference $\phi(x_1, x_2, t) - \Lambda$ between the 177

178 electric and plasma floating potentials may be neglected and,
179 second, that the parallel current losses are compensated by
180 the source $S(x_1)$ (a quasi-equilibrium hypothesis). Therefore,
181 one expects the following equations to display the same
182 qualitative behavior as those in (3):

$$\frac{\partial Ln}{\partial t} = -[\phi, Ln] - \tilde{g}\partial_2(Ln - \phi) + D(\nabla^2 Ln + |\nabla Ln|^2) \quad (4a)$$

$$\frac{\partial \nabla^2 \phi}{\partial t} = -[\phi, \nabla^2 \phi] - g\partial_2 Ln + \nu \nabla^4 \phi. \quad (4b)$$

Remark that, the source and sink terms having been dropped,
183 (4) describes a closed system, yet this does not prevent the
184 local growth of physical quantities or of their derivatives,
185 being precisely this growth, which arises from the nonlinear
186 nature of the problem, that one wants to unveil. Putting it dif-
187 ferently, the potentially dangerous concentration of mass and
188 energy in the blobs does not necessarily imply a global
189 increase of these quantities in the SOL. Then, introducing
190 the unit vector $\hat{\mathbf{b}}$ along the direction of the magnetic field
191 (the so-called parallel direction, so $\hat{\mathbf{b}} \cdot \nabla = 0$), which is such
192 that $[f, h] = \hat{\mathbf{b}} \cdot \nabla f \times \nabla h$, (4) can be rewritten as

$$\frac{\partial Ln}{\partial t} = \hat{\mathbf{b}} \cdot \nabla Ln \times \nabla \phi - \tilde{g}\partial_2(Ln - \phi) + D(\nabla^2 Ln + |\nabla Ln|^2) \quad (5a)$$

$$\frac{\partial \nabla^2 \phi}{\partial t} = \hat{\mathbf{b}} \cdot \nabla \nabla^2 \phi \times \nabla \phi - g\partial_2 Ln + \nu \nabla^4 \phi. \quad (5b)$$

193 One now assumes the solution of (5) to be defined in a
194 domain D with either periodic boundary conditions or van-
195 ishing values for all functions at its boundary, meaning, in
196 practice, that boundary terms can be dropped in all partial
197 integrations. This simplifying assumption may not seem
198 fully appropriate to the boundary between the SOL and the
199 core plasma (at $x_1 = 0$), yet any eventual nonvanishing
200 boundary terms would not be dynamical, but fixed instead,
201 and hence one does not expect them to qualitatively change
202 the inequalities obtained below. Furthermore, the growth
203 rates thus estimated are global, in that they are spatially inte-
204 grated quantities, and nonlinear, in that they proceed from
205 the model equations without any previous linearisation of the
206 latter (unlike in the approach followed below when address-
207 ing the control of fluctuations). So, multiplying (5b) by ϕ
208 and integrating over D yields [see (b) in Appendix]

$$\frac{1}{2} \frac{d}{dt} \int_D |\nabla \phi|^2 = \int_D g\phi \partial_2 Ln - \nu \int_D (\nabla^2 \phi)^2, \quad (6)$$

209 whence the inequality [see (c) in the Appendix]

$$\frac{d}{dt} \int_D |\nabla \phi|^2 \leq \int_D |\nabla Ln|^2 + \int_D (g\phi)^2, \quad (7)$$

210 which means the growth of $|\nabla \phi|$ is partially controlled by
211 the gradient $|\nabla Ln|$ of the log-density.

212 Proceeding to work out (5a) in order to establish a bound
213 on the growth of $|\nabla Ln|$, one takes the gradient of this equa-
214 tion, makes the inner product with ∇Ln , and integrates by
215 parts on the domain D to obtain [see (d) in the Appendix]

$$\begin{aligned} \frac{1}{2} \frac{d}{dt} \int_D |\nabla Ln|^2 &= -\hat{\mathbf{b}} \cdot \int_D (\nabla Ln \times \nabla \phi) \nabla^2 Ln \\ &+ \int_D \tilde{g}\partial_2(Ln - \phi) \nabla^2 Ln \\ &- \int_D D(\nabla^2 Ln + |\nabla Ln|^2) \nabla^2 Ln \end{aligned} \quad (8)$$

and, from (8), the following inequality can be derived [see 216
(e) in the Appendix] 217

$$\begin{aligned} \frac{d}{dt} \int_D |\nabla Ln|^2 &\leq \int_D |\nabla \phi|^2 + \int_D |\nabla(Ln - \phi)|^2 + \int_D D|\nabla Ln|^4 \\ &+ \int_D (\tilde{g}^2 + D + |\nabla Ln|^2)(\nabla^2 Ln)^2, \end{aligned} \quad (9)$$

or still [see (f) in the Appendix] 218

$$\begin{aligned} \frac{d}{dt} \int_D |\nabla Ln|^2 &\leq 3 \int_D |\nabla \phi|^2 + \int_D (2 + D|\nabla Ln|^2) |\nabla Ln|^2 \\ &+ \int_D (\tilde{g}^2 + D + |\nabla Ln|^2)(\nabla^2 Ln)^2. \end{aligned} \quad (10)$$

The growth of $|\nabla Ln|$ is thus bounded by $|\nabla \phi|$, whose growth
is itself bounded by $|\nabla Ln|$, suggesting a nonlinear instability 219
of the model, at least for some domains of the configuration 220
space. Admittedly, these estimates for the mutual control of 221
the log-density and the potential are estimates over global 222
integrated quantities yet, being integrals over the modulus of 223
gradients, or derivatives, an eventual growth of one such 224
integrated quantity carries information on short range varia- 225
tions, hence on local instabilities. 226

IV. CONTROL OF FLUCTUATIONS 227

Having seen in Sec. III the model may become nonli- 228
nearly unstable, the next step is to perform a linear stability 229
analysis. Indeed, the ability to control plasma behavior in 230
the SOL is highly desirable for tokamak operation, a possi- 231
ble route to achieve this being through polarisation, either of 232
the wall (biased limiter or divertor elements) or via biased 233
probes, including the injection of current by way of heated 234
emissive electrodes, both situations having been explored 235
experimentally,^{26,27} as well as numerically.^{14,17,18} Here, the 236
model in (3) will be used to understand how the control 237
of fluctuations might be achieved with the aid not only of 238
biasing, but also of magnetic-field modulation, another 239
effect worthy to be explored. So, let the source $S(x_1)$ and 240
 $V_{\text{bias}}(x_1, t)$ be such that 241

$$Ln^{(0)}(x_1) = Ln_0 - \mu^{-1}x_1 \quad (11a)$$

$$\phi^{(0)}(x_1, t) = \Lambda + V_{\text{bias}}(x_1, t) \quad (11b)$$

is a solution of (3) with Λ replaced by $\Lambda + V_{\text{bias}}(x_1, t)$, μ giv- 242
ing the scale length for the exponential decay of density in 243
the SOL. On physical grounds, one expects $V_{\text{bias}}(x_1, t)$ to be 244
of the form 245

$$V_{\text{bias}}(x_1, t) = U(x_1, t)e^{-(Z-x_1)/\lambda_D}, \quad (12)$$

Z being the radial width of the SOL in the x_1 coordinate, λ_D the Debye length, and $U(x_1, t)$ a slowly varying function of x_1 and t . The intensity $U(x_1, t)$ of the potential taken at the wall or at a probe would be a control parameter, whilst the decaying term in $V_{\text{bias}}(x_1, t)$ takes into account the screening properties of the plasma away from $x_1 = Z$. The effect of biasing is thus emulated by modifying the plasma potential around the position of the polarized element, an approach that has been standard (although using Gaussian function forms instead of (12)),^{14,17,18} but which can be replaced by more sophisticated, or “smart,” control techniques.^{32,33} One should further add that the situation conveyed by (11b) and (12) is that of a poloidally homogeneous biasing potential, which is experimentally more relevant for dealing with, say, a biased poloidal limiter, or ring, than with discrete biased probes,^{18,33} being clear that with a finite number of probes there would be in the biasing potential an x_2 -dependent modulation that would also be present in the results here derived. If one now looks for fluctuations around the unperturbed solution (11), one may write up to first order [see (g) in the Appendix],

$$Ln(x_1, x_2, t) = Ln^{(0)}(x_1) + \delta Ln(x_1, x_2, t) \quad (13a)$$

$$\phi(x_1, x_2, t) = \phi^{(0)}(x_1, t) + \delta\phi(x_1, x_2, t), \quad (13b)$$

and subsequently plug (11) and (13) into (3) to obtain

$$\frac{\partial \delta Ln}{\partial t} \simeq -\partial_1 \phi^{(0)} \partial_2 \delta Ln - \mu^{-1} \partial_2 \delta \phi - \tilde{g} \partial_2 (\delta Ln - \delta \phi) + \sigma_{\parallel} \delta \phi + D(\nabla^2 \delta Ln - 2\mu^{-1} \partial_1 \delta Ln) \quad (14a)$$

$$\frac{\partial \nabla^2 \delta \phi}{\partial t} \simeq -\partial_1 \phi^{(0)} \partial_2 \nabla^2 \delta \phi + \partial_1^3 \phi^{(0)} \partial_2 \delta \phi - g \partial_2 \delta Ln + \sigma_{\parallel} \delta \phi + \nu \nabla^4 \delta \phi. \quad (14b)$$

Next, Fourier transforming according to

$$f(x_1, x_2, t) = \frac{1}{2\pi} \iint \hat{f}(k_1, k_2, t) e^{i(k_1 x_1 + k_2 x_2)} dk_1 dk_2, \quad (15)$$

(14) becomes

$$\frac{\partial \widehat{\delta Ln}}{\partial t} \simeq -(Dk^2 + i2D\mu^{-1}k_1 + i\tilde{g}k_2) \widehat{\delta Ln} - [i(\mu^{-1} - \tilde{g})k_2 - \sigma_{\parallel}] \widehat{\delta \phi} - \frac{1}{2\pi} (\widehat{\partial_1 \phi^{(0)}} * \partial_2 \widehat{\delta Ln}) \quad (16a)$$

$$\frac{\partial \widehat{\delta \phi}}{\partial t} \simeq i \frac{gk_2}{k^2} \widehat{\delta Ln} - \left[\nu k^2 + \frac{\sigma_{\parallel}}{k^2} \right] \widehat{\delta \phi} + \frac{1}{2\pi k^2} (\widehat{\partial_1 \phi^{(0)}} * \partial_2 \nabla^2 \widehat{\delta \phi}) - \frac{1}{2\pi k^2} (\widehat{\partial_1^3 \phi^{(0)}} * \partial_2 \widehat{\delta \phi}), \quad (16b)$$

with $k = \sqrt{k_1^2 + k_2^2}$. The convolution products that appear in (16) of the form

$$\frac{1}{2\pi} (\widehat{f} * \widehat{h})(k_1, k_2, t) = \frac{1}{2\pi} \iint \hat{f}(q_1, q_2, t) \widehat{h}(k_1 - q_1, k_2 - q_2, t) dq_1 dq_2 \quad (17)$$

can be rewritten, with recourse to (15), as

$$\frac{1}{2\pi} (\widehat{f} * \widehat{h})(k_1, k_2, t) = \frac{1}{4\pi^2} \iiint f(x_1, x_2, t) \widehat{h}(k_1 - q_1, k_2 - q_2, t) e^{-i(q_1 x_1 + q_2 x_2)} dx_1 dx_2 dq_1 dq_2, \quad (18)$$

yielding upon expansion [see (h) in the Appendix]

$$\frac{1}{2\pi} (\widehat{f} * \widehat{h})(k_1, k_2, t) = \iint \sum_{n=0}^{\infty} \sum_{n'=0}^{\infty} \frac{(x_1 \partial_1 + x_2 \partial_2)^n f(0, 0, t)}{n!} \frac{(-i)^{n'} (\partial_1 \partial_{k_1} + \partial_2 \partial_{k_2})^{n'} \widehat{h}(k_1, k_2, t)}{n'} \delta(x_1) \delta(x_2) dx_1 dx_2, \quad (19)$$

with $\partial_{ki} = \partial / \partial k_i$, (19) being equivalent to [see (i) in the Appendix]

$$\frac{1}{2\pi} (\widehat{f} * \widehat{h})(k_1, k_2, t) = \sum_{n=0}^{\infty} \frac{i^n (\partial_1 \partial_{k_1} + \partial_2 \partial_{k_2})^n f(0, 0, t) \widehat{h}(k_1, k_2, t)}{n!}, \quad (20)$$

or, in operator form, to

$$\frac{1}{2\pi} (\widehat{f} * \widehat{h})(k_1, k_2, t) = e^{i\nabla \cdot \nabla_k} f(0, 0, t) \widehat{h}(k_1, k_2, t), \quad (21)$$

after defining $\nabla_k = (\partial_{k_1}, \partial_{k_2})$. Keeping only the leading, lowest-order term in (21) and making, for short, $f_0 = f(0, 0, t)$, (16) becomes

$$\frac{\partial \widehat{\delta Ln}}{\partial t} \simeq -[Dk^2 + i2D\mu^{-1}k_1 + i(\tilde{g} + \partial_1 \phi_0^{(0)})k_2] \widehat{\delta Ln} - [i(\mu^{-1} - \tilde{g})k_2 - \sigma_{\parallel}] \widehat{\delta \phi} \quad (22a)$$

$$\frac{\partial \widehat{\delta\phi}}{\partial t} \simeq i \frac{gk_2}{k^2} \widehat{\delta Ln} - \left[\nu k^2 + i \left(\partial_1 \phi_0^{(0)} + \frac{\partial_1^3 \phi_0^{(0)}}{k^2} \right) k_2 + \frac{\sigma_{||}}{k^2} \right] \widehat{\delta\phi}. \quad (22b)$$

The damping/growth rates for the fluctuation modes follow from solving the characteristic equation for the system (22) of two linear ordinary differential equations (ODE's), whose solutions are [see (j) in Appendix]

$$\lambda_{\pm} \simeq -\frac{1}{2} \left[(D + \nu)k^2 + i2D\mu^{-1}k_1 + i \left(\tilde{g} + 2\partial_1 \phi_0^{(0)} + \frac{\partial_1^3 \phi_0^{(0)}}{k^2} \right) k_2 + \frac{\sigma_{||}}{k^2} \right] \pm \frac{1}{2} \sqrt{\left[(\nu - D)k^2 - i2D\mu^{-1}k_1 - i \left(\tilde{g} - \frac{\partial_1^3 \phi_0^{(0)}}{k^2} \right) k_2 + \frac{\sigma_{||}}{k^2} \right]^2 - i \frac{4gk_2}{k^2} \left[ik_2(\mu^{-1} - \tilde{g}) - \sigma_{||} \right]}, \quad (23)$$

which can be seen to become equivalent to the FDUT dispersion relation found in the literature if one further assumes $k_1 \simeq 0$ and a uniform $\phi_0^{(0)}$.^{15,34} Provided D , ν , and $\sigma_{||}$ are small enough to make $D \simeq \nu \simeq \sigma_{||} \simeq 0$, (23) reads

$$\lambda_{\pm} \simeq -\frac{i}{2} \left(\tilde{g} + 2\partial_1 \phi_0^{(0)} + \frac{\partial_1^3 \phi_0^{(0)}}{k^2} \right) k_2 \pm \frac{|k_2|}{2k} \sqrt{4g(\mu^{-1} - \tilde{g}) - \left(\tilde{g}k - \frac{\partial_1^3 \phi_0^{(0)}}{k} \right)^2}, \quad (24)$$

yielding the damping/growth rates

$$\gamma_{\pm} \simeq \pm \frac{|k_2|}{2k} \sqrt{4g(\mu^{-1} - \tilde{g}) - \left(\tilde{g}k - \frac{\partial_1^3 \phi_0^{(0)}}{k} \right)^2}, \quad (25)$$

whenever the quantity under the square root is non-negative. Therefore, from (25), the solutions of (22) will not grow indefinitely (and become unstable) provided

$$4g(\mu^{-1} - \tilde{g})k^2 \leq (\tilde{g}k^2 - \partial_1^3 \phi_0^{(0)})^2, \quad (26)$$

which thus reads as a condition for stability. Condition (26) clearly recovers the driving effect (*vis-à-vis* instability) of a negative density gradient (a positive μ), as well as the stabilising role of the third derivative of the potential, in accordance with the previous results obtained for the interchange instability in the SOL with $\tilde{g} = 0$.¹⁴ It is a first-order condition, secured by keeping only the leading term in the convolution-product expansions (20) or (21), and better approximations can be derived using higher-order terms in those expansions.

Now, a physical argument allows for an accurate interpretation of (26) if, referring to the form (12) for the biasing potential, one notices, from (11), that $\phi_0^{(0)} = \Lambda + U_0 e^{-Z/\lambda_D}$ is the potential at a distance Z from the polarisation probe. Hence, introducing the distance to the probe as a parameter, recalling (2) and (11), assuming a negative density gradient in the SOL, and neglecting the derivatives of the slowly varying $U(x_1, t)$ in (12), criterion (26) can be expressed in terms of physical variables as

$$4k^2 \partial_1 \left(\frac{1}{B} \right) \left[\frac{|\partial_1 n|}{n} - \partial_1 \left(\frac{1}{B} \right) \right] \leq \left[k^2 \partial_1 \left(\frac{1}{B} \right) - \frac{U_0 e^{-Z/\lambda_D}}{\lambda_D^3} \right]^2. \quad (27)$$

Regarding controllability, one may infer the following conclusions from (27):³⁵ control of unstable modes is a local effect, and becomes increasingly difficult further away from the probe (because of the e^{-Z/λ_D} term); a negative polarisation intensity U_0 is more favorable than a positive one (accounting for the fact that, in general, $\partial_1(1/B) \geq 0$ in a tokamak), whereas for positive U_0 the less controllable modes occur around $k^2 \simeq U_0 e^{-Z/\lambda_D} / \lambda_D^3 \partial_1(1/B)$; decreasing the magnetic-field inhomogeneity increases controllability, suggesting that making the magnetic field in the SOL as uniform as possible (so has to have $\partial_1(1/B) \approx 0$ there) may reduce turbulence. The simplest way of achieving this is to increase the strength B of the magnetic field, namely, of its dominant toroidal component which, by reducing the plasma normalized pressure (the so-called plasma β), is also good for its macroscopic, magnetohydrodynamic (MHD) stability, the disadvantage being a potentially higher cost for the magnetic coils.³⁶ In agreement with the advantage here predicted of using a negative U_0 , it is worth saying that experiments have indeed shown that negative biasing leads not only to a larger improvement in particle confinement, but it also reduces the propagation of large-scale events (or blobs) and lowers the amplitude of fluctuations.^{26,27} Note that such a prediction, on being more beneficial to apply a negative (as opposed to a positive) bias, could not be retrieved from the TOKAM-2D model because $\tilde{g} = 0$ there,^{12-14,17,18,37} and with $\tilde{g} = 0$ (27) would read $4k^2 \partial_1(1/B) |\partial_1 n| / n \leq (U_0 e^{-Z/\lambda_D} / \lambda_D^3)^2$ instead, a condition where the sign of U_0 has no influence whatsoever. It could also not be retrieved from the dispersion relation previously established in connection with FDUT simulations, even if the latter properly allowed for a finite, non-vanishing \tilde{g} , as neither biasing nor a non-uniform unperturbed potential $\phi_0^{(0)}$ were explicitly accounted for ($\phi_0^{(0)}$ having been set to the electron temperature, obviously uniform in the FDUT model).¹⁵ Note still that the linear growth rate for the interchange instability has been known to be an increasing function of the radial decay

334 of the magnetic field as conveyed by g on the lhs of (26),¹⁴
 335 but the discussion now becomes more subtle because of the
 336 presence of \tilde{g} , so much so that for asymptotically large
 337 magnetic-field inhomogeneities (so as to render negligible
 338 both the density and vorticity gradients) the system does
 339 become stable, with linear stability becoming independent of
 340 $\partial_1(1/B)$. Before concluding this section, it is worth pointing
 341 out that any dependence of the biasing on x_2 (for instance,
 342 coming from using a finite number of localized probes),^{18,33}
 343 and the subsequent modulation on this variable it would
 344 entail in the results derived above, would not invalidate the
 345 conclusions drawn concerning the asymmetric effect of
 346 positive and negative electric bias and the smoothing of the
 347 magnetic-field inhomogeneity.

348 **V. STRUCTURES AND CONSERVATIVE DYNAMICS**

349 Having up to now been concerned, in Secs. III and IV,
 350 with growth rates and the stability (both linear and nonlinear)
 351 of model solutions, it is time to try to retrieve some of the fea-
 352 tures of the solutions themselves. Many dynamical systems
 353 of physical interest have both conservative and dissipative
 354 components, having been proved that the finite-dimensional
 355 vector fields always correspond to a superposition of
 356 Hamiltonian and gradient components.²⁸ The identification of
 357 the Hamiltonian component is important because it frequently
 358 happens that, in some regions of phase space, the effect of the
 359 non-conservative components cancels out along a neighbour-
 360 hood of some of the Hamiltonian orbits, implying the full sys-
 361 tem ends up displaying deformed versions of the latter, which
 362 led to the notion of “constants of motion in dissipative sys-
 363 tems.”³⁸ It is conceivable that a similar situation might apply
 364 in infinite dimensions because one of the tools used for the
 365 finite-dimensional vector field decomposition, namely, the
 366 Hodge–De Rahm theorem, can be extended to infinite dimen-
 367 sions.³⁹ For the physical problem dealt with in this paper, the
 368 implication is that, looking for solutions of the conservative
 369 part of the model, one might at least obtain the ancestors of
 370 coherent structures that might also exist in the full model.

371 Therefore, going back to the model in (3), its conserva-
 372 tive part reads as the system of partial differential equations
 373 (PDE’s)

$$\frac{\partial Ln}{\partial t} = -[\phi, Ln] - \tilde{g}\partial_2(Ln - \phi) \quad (28a)$$

$$\frac{\partial \nabla^2 \phi}{\partial t} = -[\phi, \nabla^2 \phi] - g\partial_2 Ln, \quad (28b)$$

374 which, upon the transformation

$$Ln(x_1, x_2, t) = \tilde{Ln}(x_1, x_2, t) - \tilde{g}x_1 \quad (29a)$$

$$\phi(x_1, x_2, t) = \tilde{\phi}(x_1, x_2, t) - \tilde{g}x_1 \quad (29b)$$

375 and assuming \tilde{g} to be constant (hence also g because of (2)),
 376 becomes

$$\frac{\partial \tilde{Ln}}{\partial t} = -[\tilde{\phi}, \tilde{Ln}] \quad (30a)$$

$$\frac{\partial \nabla^2 \tilde{\phi}}{\partial t} = -[\tilde{\phi}, \nabla^2 \tilde{\phi}] - g\partial_2 \tilde{Ln} + \tilde{g}\partial_2 \nabla^2 \tilde{\phi}. \quad (30b)$$

One now looks for travelling-wave solutions to this system
 by writing 377

$$\tilde{Ln}(x_1, x_2, t) = \tilde{Ln}(x_1 - v_1 t, x_2 - v_2 t) \quad (31a)$$

$$\tilde{\phi}(x_1, x_2, t) = \tilde{\phi}(x_1 - v_1 t, x_2 - v_2 t) \quad (31b)$$

so that, defining $y_i = x_i - v_i t$ and making $\partial_i = \partial/\partial y_i$ hence-
 forth, one obtains from (30) and (31) 378
379

$$v_1 \partial_1 \tilde{Ln} + v_2 \partial_2 \tilde{Ln} = \partial_1 \tilde{\phi} \partial_2 \tilde{Ln} - \partial_1 \tilde{Ln} \partial_2 \tilde{\phi} \quad (32a)$$

$$v_1 \partial_1 \nabla^2 \tilde{\phi} + v_2 \partial_2 \nabla^2 \tilde{\phi} = \partial_1 \tilde{\phi} \partial_2 \nabla^2 \tilde{\phi} - \partial_1 \nabla^2 \tilde{\phi} \partial_2 \tilde{\phi} + g\partial_2 \tilde{Ln} - \tilde{g}\partial_2 \nabla^2 \tilde{\phi}. \quad (32b)$$

Putting 380

$$\tilde{\phi}(y_1, y_2) = F(y_1, y_2) + v_2 y_1 - v_1 y_2, \quad (33)$$

(32a) reduces to 381

$$\partial_1 F \partial_2 \tilde{Ln} = \partial_1 \tilde{Ln} \partial_2 F \quad (34a)$$

$$\partial_1 F \partial_2 \nabla^2 F - \partial_1 \nabla^2 F \partial_2 F = -g\partial_2 \tilde{Ln} + \tilde{g}\partial_2 \nabla^2 F, \quad (34b)$$

where (34a) can be seen to be satisfied for 382

$$\tilde{Ln} = f(F), \quad (35)$$

with f an arbitrary differentiable function, so substitution in
 (34b) yields 383
384

$$\partial_1 F \partial_2 \nabla^2 F - \partial_1 \nabla^2 F \partial_2 F + g\partial_2 f(F) - \tilde{g}\partial_2 \nabla^2 F = 0, \quad (36)$$

which admits a very large number of solutions, depending on
 the choice of $f(F)$. The symmetry exhibited by (34) allows
 one to identify also as solutions those of the form 385
386
387

$$F(y_1, y_2) = F_s(y_1, y_2) \quad (37)$$

and 388

$$\tilde{Ln} = \Theta_s F_s, \quad (38)$$

with Θ_s and F_s , respectively, an operator and a function
 symmetric in y_1 and y_2 (meaning they remain invariant under
 an exchange between the two variables), so 389
390
391

$$F_s(y_2, y_1) = F_s(y_1, y_2) \quad (39)$$

and 392

$$\Theta_s F_s(y_2, y_1) = \Theta_s F_s(y_1, y_2), \quad (40)$$

in which case (34) becomes 393

$$g\partial_2 \Theta_s F_s - \tilde{g}\partial_2 \nabla^2 F_s = 0. \quad (41)$$

For example, possible solutions obeying (35) can be
 obtained by making 394
395

$$f(F) = \alpha F, \tag{42}$$

396 with α constant, and writing

$$F(y_1, y_2) = \tilde{F}(y_1, y_2) + \tilde{g}y_1, \tag{43}$$

397 so (36) takes the form

$$\partial_1 \tilde{F} \partial_2 \nabla^2 \tilde{F} - \partial_1 \nabla^2 \tilde{F} \partial_2 \tilde{F} = -\alpha \tilde{g} \partial_2 \tilde{F}. \tag{44}$$

398 An obvious solution to the homogeneous counterpart of (44)
399 (obtained by setting to zero the rhs of the latter) is the wave
form [see (k) in the Appendix]

$$\tilde{F}_0(y_1, y_2) = A \cos(k_1 y_1 + k_2 y_2) + B \sin(k_1 y_1 + k_2 y_2) \tag{45}$$

400 and, plugging into (44), the *ansatz*

$$\tilde{F}(y_1, y_2) = \tilde{F}_0(y_1, y_2) + H(y_1), \tag{46}$$

401 chosen such as not to introduce an extra term on the rhs of
402 (44), one gets, already accounting for (45),

$$[(k^2 + \partial_1^2) \partial_1 H - \alpha \tilde{g}] \partial_2 \tilde{F}_0 = 0. \tag{47}$$

To solve the ODE on the lhs of (47), one may transform it into a homogeneous ODE by setting

$$H(y_1) = \tilde{H}(y_1) + \frac{\alpha \tilde{g}}{k^2} y_1, \tag{48}$$

so

$$\partial_1^3 \tilde{H} + k^2 \partial_1 \tilde{H} = 0, \tag{49}$$

whose solution is trivially found to be [see (l) in the Appendix]

$$\tilde{H}(y_1) = C_0 + C_1 \cos(ky_1) + C_2 \sin(ky_1). \tag{50}$$

Retracing the calculation backwards and assembling together (29), (31), (33), (35), (42), (43), (45), (46), (48), and (50), the original quantities that are solutions to (28) are thus

$$Ln(x_1, x_2, t) = \alpha[\phi(x_1, x_2, t) - v_2(x_1 - v_1 t) + v_1(x_2 - v_2 t)] + (\alpha - 1)\tilde{g}x_1 \tag{51a}$$

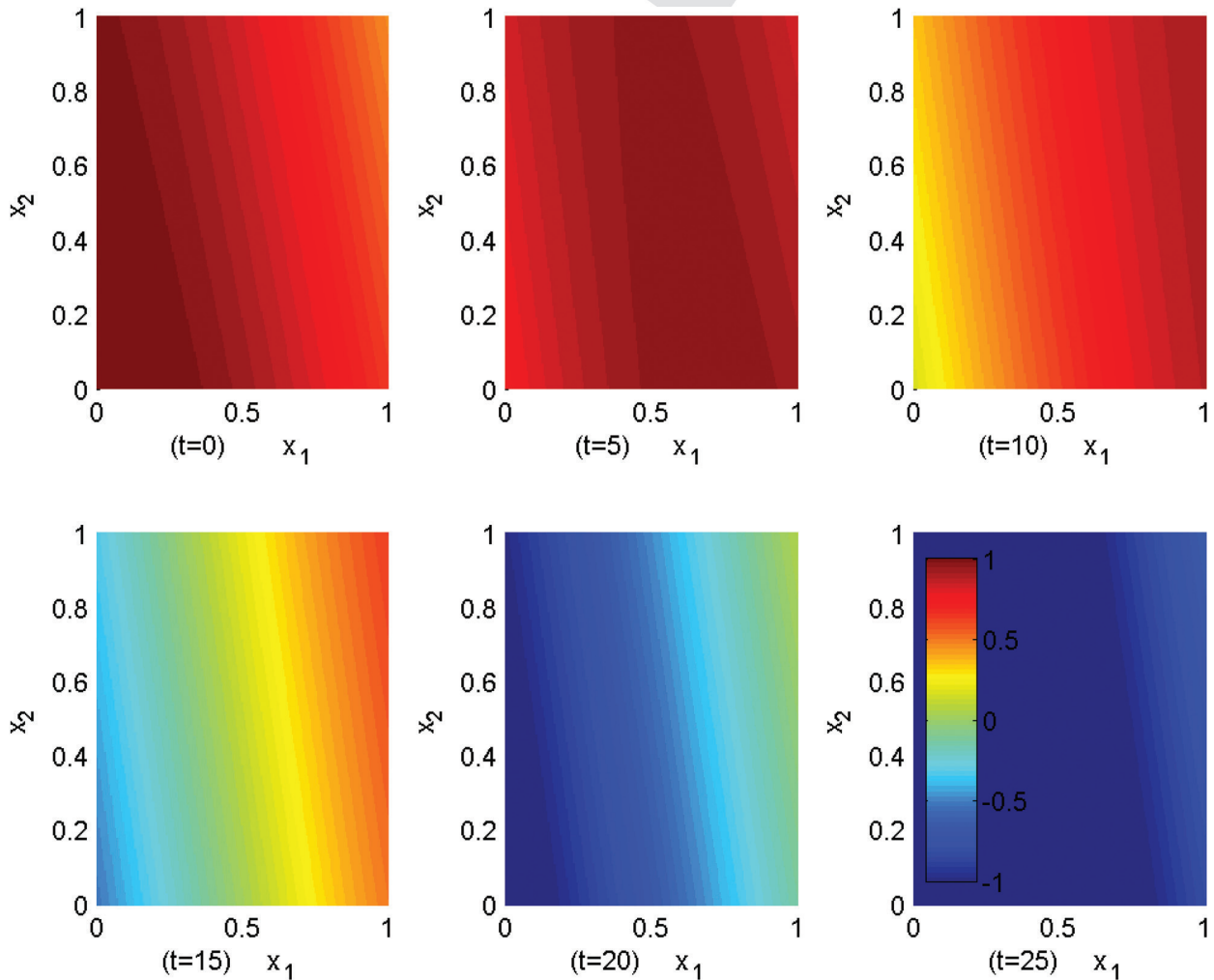


FIG. 1. Six snapshots with contour plots of the log-density function Ln for the solution (51) of the conservative system (28), with $B = C_0 = C_1 = C_2 = 0$, $\alpha = A = 1$, $v_1 = v_2 = 0.1$, $k_1 = 1$, $k_2 = 0.2$, and $g = \tilde{g} = 0.1$, the units in the colour bar being arbitrary.

$$\begin{aligned} \phi(x_1, x_2, t) = & \left(v_2 + \tilde{g} + \frac{\alpha g}{k^2} \right) (x_1 - v_1 t) - v_1 (x_2 - v_2 t) - \tilde{g} x_1 \\ & + A \cos[k_1 (x_1 - v_1 t) + k_2 (x_2 - v_2 t)] \\ & + B \sin[k_1 (x_1 - v_1 t) + k_2 (x_2 - v_2 t)] \\ & + C_0 + C_1 \cos[k(x_1 - v_1 t)] + C_2 \sin[k(x_1 - v_1 t)]. \end{aligned} \tag{51b}$$

In Fig. 1 are shown snapshots of the propagation of the function $Ln(x_1, x_2, t)$ for one such solution with $B = C_0 = C_1 = C_2 = 0$, $\alpha = A = 1$, $v_1 = v_2 = 0.1$, $k_1 = 1, k_2 = 0.2$, and $g = \tilde{g} = 0.1$, and one clearly sees how the wave front propagates from the inner boundary (the core plasma region) to the outer layer. Of course, solutions of (36) such as (51) are only solutions to the conservative part of the equations, with diffusion, parallel losses, and source not being accounted for. However, inspection of (3) suggests the role of the unspecified source term in (3a) is to compensate for the parallel losses, whereas the longitudinal conductance term in (3b) will not play a determinant role as long as fluctuations away from the plasma potential are not very large. Therefore, it is not unlikely that the overall structure of the

complete solutions will be mostly determined by the conservative dynamics induced by (28).

Another solution to the homogeneous counterpart of (44) is

$$\tilde{F}_0(y_1, y_2) = Ae^{(k_1 y_1 + k_2 y_2)}, \tag{52}$$

hence, putting

$$\tilde{F}(y_1, y_2) = \tilde{F}_0(y_1, y_2) + \tilde{H}(y_1) - \frac{\alpha g}{k^2} y_1, \tag{53}$$

(44) becomes

$$\partial_1^3 \tilde{H} - k^2 \partial_1 \tilde{H} = 0, \tag{54}$$

whose general solution reads [see (m) in the Appendix]

$$\tilde{H}(y_1) = C_0 + C_1 e^{ky_1} + C_2 e^{-ky_1}. \tag{55}$$

On account of this, the functions

$$\begin{aligned} Ln(x_1, x_2, t) = & \alpha[\phi(x_1, x_2, t) - v_2(x_1 - v_1 t) + v_1(x_2 - v_2 t)] \\ & + (\alpha - 1)\tilde{g}x_1 \end{aligned} \tag{56a}$$

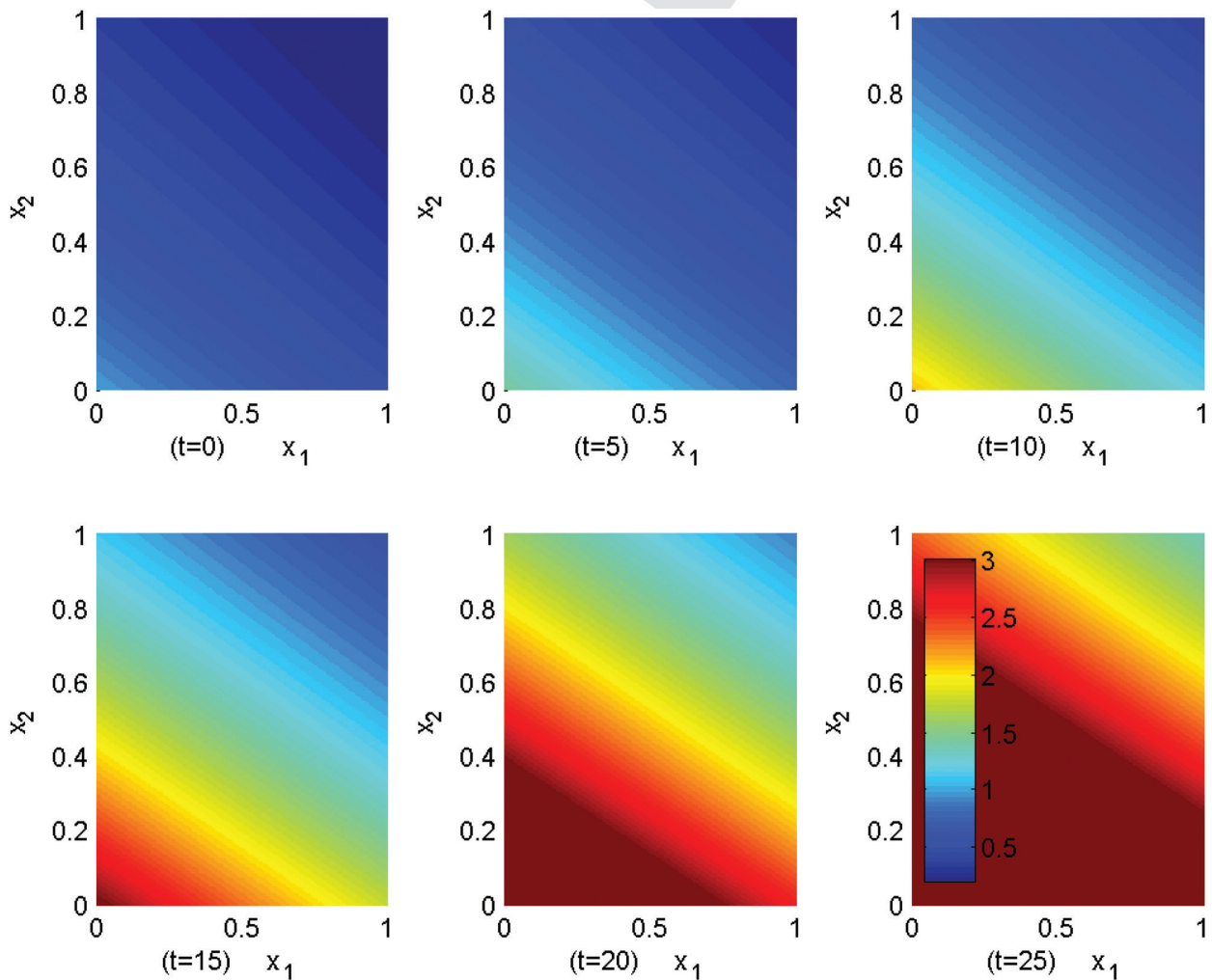


FIG. 2. Six snapshots with contour plots of the log-density function Ln for the solution (56) of the conservative system (28), for $C_0 = C_1 = C_2 = 0$, $\alpha = A = 1, v_1 = v_2 = 0.05, k_1 = -0.5, k_2 = -1$, and $g = \tilde{g} = 0.1$, the units in the colour bar being arbitrary.

$$\begin{aligned} \phi(x_1, x_2, t) = & \left(v_2 + \tilde{g} - \frac{\alpha g}{k^2} \right) (x_1 - v_1 t) - v_1 (x_2 - v_2 t) - \tilde{g} x_1 \\ & + A e^{[k_1(x_1 - v_1 t) + k_2(x_2 - v_2 t)]} + C_0 + C_1 e^{k(x_1 - v_1 t)} \\ & + C_2 e^{-k(x_1 - v_1 t)} \end{aligned} \quad (56b)$$

431 are also solutions to (28), snapshots of $Ln(x_1, x_2, t)$ hereabove
 432 being given in Fig. 2 for $C_0 = C_1 = C_2 = 0$, $\alpha = A = 1$,
 433 $v_1 = v_2 = 0.05$, $k_1 = -0.5$, $k_2 = -1$, and $g = \tilde{g} = 0.1$. One
 434 sees, also in this case, a large-scale structure that is initially
 435 located at the inner SOL region and subsequently starts mov-
 436 ing essentially outwards. The important point to retain here is
 437 the existence of solutions that move concentrations of parti-
 438 cles and energy along both (radial- and poloidal-like) direc-
 439 tions in a 2D cross-section, eventually ejecting them from the
 440 core to the wall, hence mimicking the basic, gross behavior
 441 depicted by blobs that is observed in experiments and numeri-
 442 cal simulations.^{2,4,6,9-11,14-16,19-22}

443 Eventually more localized solutions to (28) can be
 444 derived from (41) by noting that the Laplacian operator ∇^2
 445 is symmetric in y_1 and y_2 , so one can put

$$\Theta_s F_s = \frac{\tilde{g}}{g} \nabla^2 F_s \quad (57)$$

and choose (amongst very many possibilities)

$$F_s(y_1, y_2) = A e^{-\gamma(y_1^2 + y_2^2)/2}, \quad (58)$$

which leads to

$$\begin{aligned} Ln(x_1, x_2, t) = & -\frac{\tilde{g}}{g} \gamma A e^{-\gamma[(x_1 - v_1 t)^2 + (x_2 - v_2 t)^2]/2} \\ & \times \left\{ 2 - \gamma \left[(x_1 - v_1 t)^2 + (x_2 - v_2 t)^2 \right] \right\} - \tilde{g} x_1 \end{aligned} \quad (59a)$$

$$\begin{aligned} \phi(x_1, x_2, t) = & A e^{-\gamma[(x_1 - v_1 t)^2 + (x_2 - v_2 t)^2]/2} \\ & + v_2 (x_1 - v_1 t) - v_1 (x_2 - v_2 t) - \tilde{g} x_1 \end{aligned} \quad (59b)$$

by back substituting through (29), (31), (33), (37), (38), (57),
 448 and (58). The time evolution of $Ln(x_1, x_2, t)$ given by (59)
 449 is shown in Fig. 3 for $A = -1.0$, $v_1 = 0.048$, $v_2 = 0.028$,
 450 $\gamma = 15$, and $g = \tilde{g} = 0.1$, and in Fig. 4 for the same set of
 451 parameters but for $\gamma = 50$. The shape of the blob-like struc-
 452 tures depicted in Figs. 3 and 4 can be modulated by multiply-
 453 ing the Gaussian packet in (58) by any other function
 454 symmetric in y_1 and y_2 , which can take a multitude of
 455

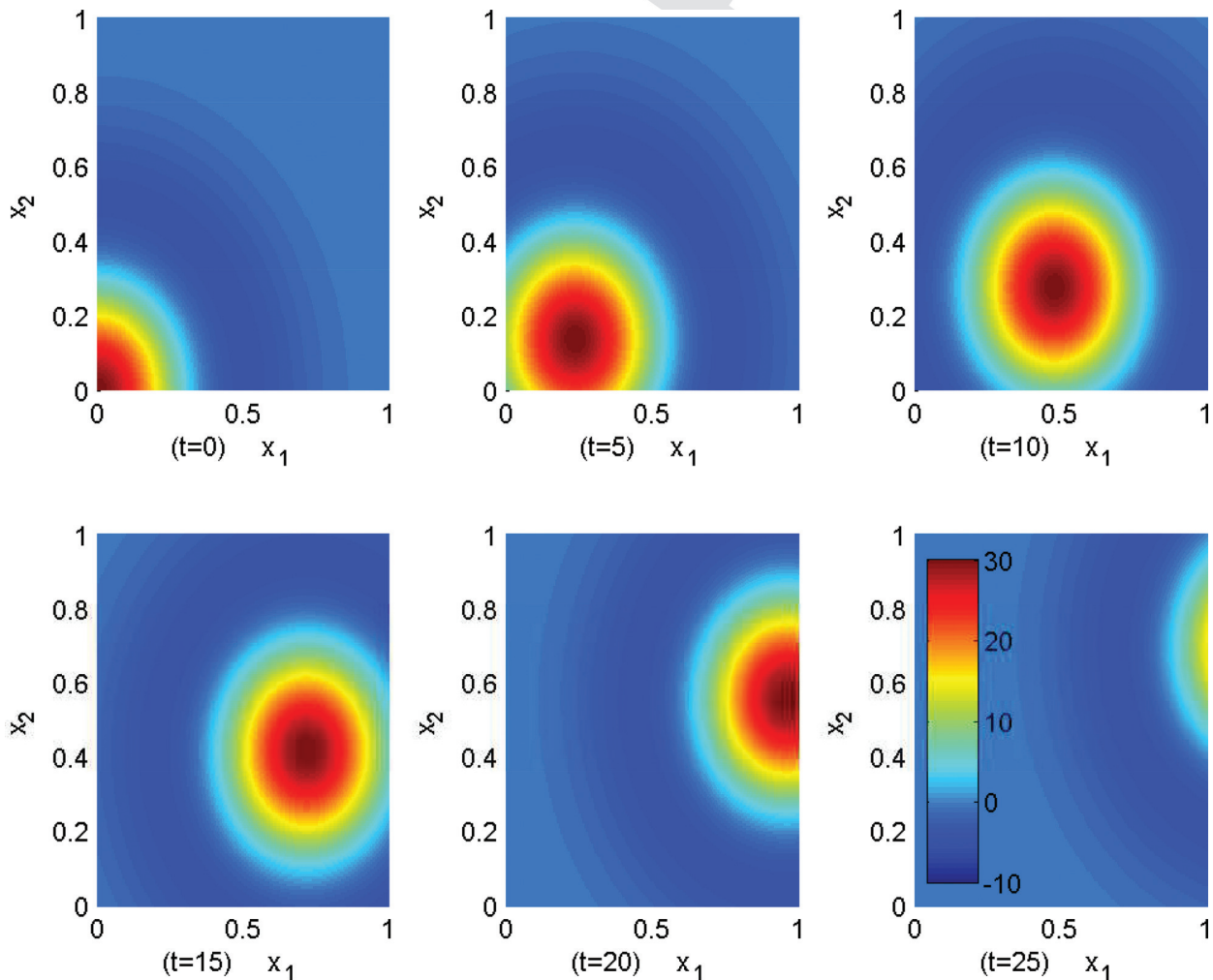


FIG. 3. Six snapshots with contour plots of the log-density function Ln for the solution (59) of the conservative system (28), for $A = -1.0$, $v_1 = 0.048$, $v_2 = 0.028$, $\gamma = 15$, and $g = \tilde{g} = 0.1$, the units in the colour bar being arbitrary.

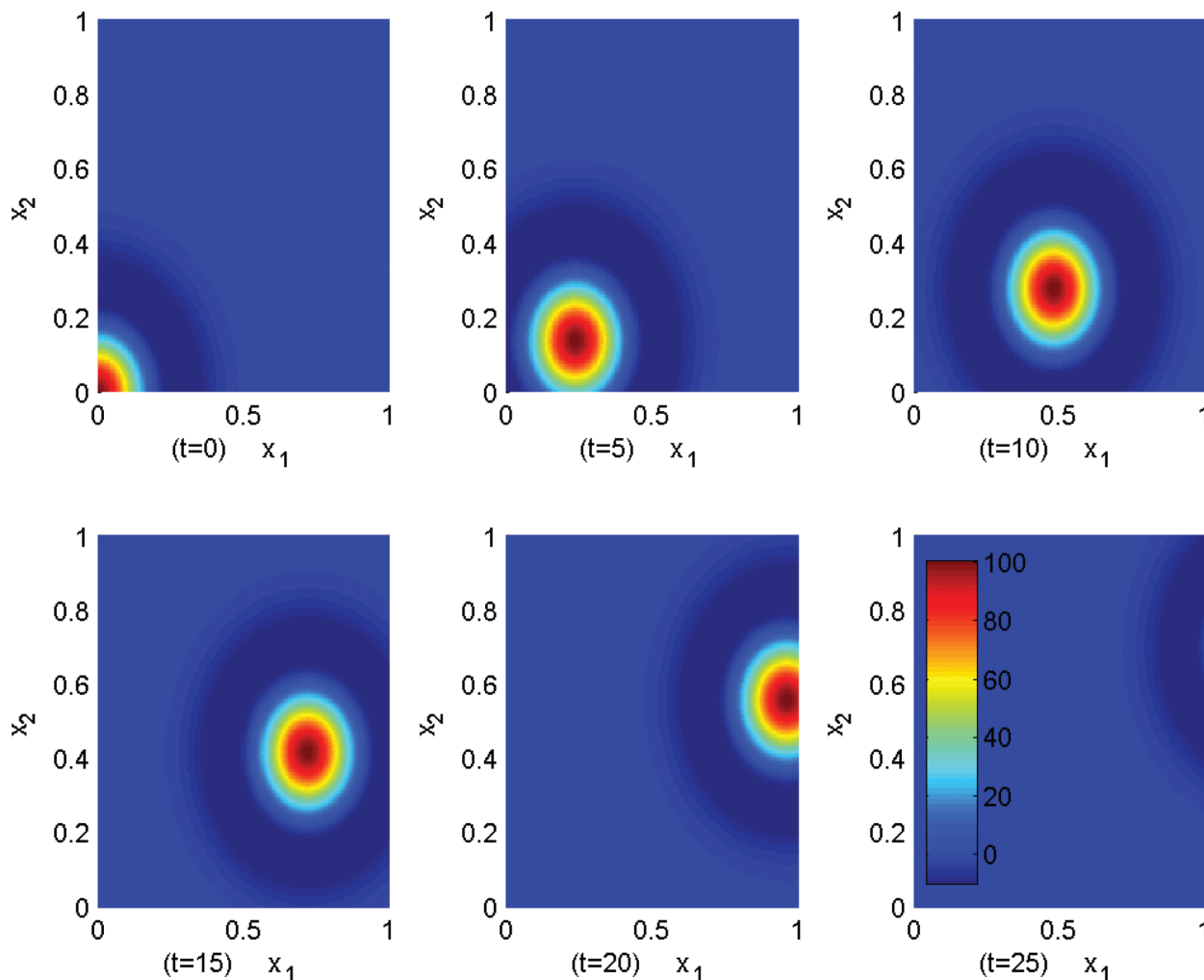


FIG. 4. Six snapshots with contour plots of the log-density function L_n for the solution (59) of the conservative system (28), for $A = -1.0$, $v_1 = 0.048$, $v_2 = 0.028$, $\gamma = 50$, and $g = \bar{g} = 0.1$, the units in the colour bar being arbitrary.

456 different forms including, for instance, polynomial or trigo-
 457 nometric. As exemplified in Figs. 1–4 for solutions (51),
 458 (56), and (59), the blob-, jet-like behavior of large-scale
 459 structures arising from solving for the conservative part of
 460 the model can take very many distinct forms, in fact, as
 461 many as afforded by the very large number of possible solu-
 462 tions to (28), combined with the multiplicity in the choice of
 463 the various parameters characterizing them. Before conclud-
 464 ing, note the plots in Figs. 1–4 have no pretension, at this
 465 stage, to exactly mimic or reproduce any actual experimental
 466 observations, and some of them may even end up by not
 467 being easily associated with a physical picture of what hap-
 468 pens in the SOL. Strictly speaking, they represent exact solu-
 469 tions of a system of PDE's, some of which may not have an
 470 obvious physical interpretation, a direct confrontation with
 471 experiments demanding eventually a more judicious choice
 472 of the parameters entering them which, probably, have to be
 473 chosen taking into account appropriate initial or boundary
 474 conditions, as well as the relevant machine data.

475 VI. SUMMARY AND CONCLUSIONS

476 In this article, a theoretical analysis has been provided
 477 on various mathematical aspects of a two-fluid model

describing SOL turbulence in slab geometry, similar to the 478
 TOKAM-2D model,^{12–14,17,18} but retaining the magnetic- 479
 field inhomogeneity terms in the continuity equation as in 480
 previous FDUT simulations.^{15,16} The model equations have 481
 a conservative kernel governing transport across magnetic- 482
 field lines, plus extra terms that account for diffusion, longi- 483
 tudinal losses (along the magnetic field) and a plasma core 484
 source. It has been shown that an upper bound for the growth 485
 rate of the vorticity gradient depends on (hence is partially 486
 controlled by) the density gradient and that, inversely, an 487
 upper bound for the growth rate of the latter depends on the 488
 former, which seems to indicate the presence in the model of 489
 a nonlinear instability, with both quantities working together 490
 to pull their gradients further and further up. The possibility 491
 of controlling the turbulent fluctuations in model quantities 492
 by means of a biasing potential has also been assessed, hav- 493
 ing one confirmed the stabilising role played by the third 494
 derivative of this potential,¹⁴ but also having one demon- 495
 strated that negative is more favorable than positive bias, 496
 thus providing a theoretical explanation for the experimental 497
 observations pointing in the same direction.^{26,27} In relation 498
 to the benefits of applying a negative versus a positive polar- 499
 ization, it is worth mentioning that it has quite recently been 500

found that a negative electrode biasing stabilizes the $m/n = 2/1$ tearing mode, by accelerating its rotation, whereas a positive biasing leads to opposite effects.⁴⁰ It has further been checked that reducing the inhomogeneity of the magnetic field in the SOL helps in stabilizing fluctuations there. Keep in mind that it is not within the scope of this paper to address the eventual use of finer, “smarter” control techniques, nor their eventual energetic cost,^{32,33} its purpose regarding control of fluctuations being limited to the more “brute-force” approach of identifying how one could act on the stability of possible turbulent modes and on their growth rates, so as to compare with the previous linear-stability-analysis results.¹⁴

Finally, the model equations have been analytically solved for their conservative part and exact solutions of the travelling-wave type have been derived, some of which propagate from the inner to the outer plasma layers and might, therefore, be interpreted as the conservative ancestors of the collective, large-scale structures named blobs observed both in experiments and in computations. Of course, this plausible conjecture that the exact travelling-wave solutions of the conservative model are the ancestors of the collective local structures that develop in the SOL should be confirmed for the full model by numerical simulations. This is a project under development for which, as stated in Sec. I, to have already some analytical control over model solutions will allow one to distinguish between the actual model behavior and the numerical artefacts or nonsense.

ACKNOWLEDGMENTS

The authors thank Rogério Jorge and Patrick Tamain for useful comments on the manuscript, and are also grateful to Luís Venâncio for identifying some errors in the original plots.

This work was carried out within the framework of the EUROfusion Consortium and received funding from the Euratom research and training programme 2014–2018 under Grant Agreement No. 633053, including enabling the research project CfP-WP14-ER-01/CEA-09. Instituto Superior Técnico (IST) activities also received financial support from Fundação para a Ciência e a Tecnologia (FCT, Lisboa) through project No. UID/FIS/50010/2013. The views and opinions expressed herein do not necessarily reflect those of the European Commission, of FCT, of IST or of their services.

APPENDIX: COMPLEMENTARY MATHEMATICAL DETAILS

- (a) Note that the diffusion related term $D|\nabla Ln|^2$ in (3), which is often missing in SOL literature, comes from the usual $D\nabla^2 n$ term in the equation for $\partial n/\partial t$, which transforms according to $D\nabla^2 n/n = D(\nabla^2 Ln + |\nabla Ln|^2)$ when passing to the equation for $\partial Ln/\partial t$.
- (b) Note that $\int_D \phi \partial \nabla^2 \phi / \partial t = -\int_D \nabla \phi \cdot \partial \nabla \phi / \partial t = -(1/2) \int_D \partial |\nabla \phi|^2 / \partial t$ and $\int_D \phi \nabla \nabla^2 \phi \times \nabla \phi = -\int_D \nabla \times (\phi \nabla \phi) \nabla^2 \phi = -\int_D (\phi \nabla \times \nabla \phi + \nabla \phi \times \nabla \phi) \nabla^2 \phi = 0$.

- (c) Note that $\nu(\nabla^2 \phi)^2 \geq 0$, $(g\phi - \partial_2 Ln)^2 \geq 0$, so $2\phi g \partial_2 Ln \leq (g\phi)^2 + (\partial_2 Ln)^2$, and $(\partial_2 Ln)^2 \leq (\partial_2 Ln)^2 + (\partial_1 Ln)^2 = |\nabla Ln|^2$.
- (d) Note that $\int_D \nabla Ln \cdot \partial \nabla Ln / \partial t = (1/2) \int_D \partial |\nabla Ln|^2 / \partial t$, $\int_D \nabla Ln \cdot \nabla (\hat{\mathbf{b}} \cdot \nabla Ln \times \nabla \phi) = -\hat{\mathbf{b}} \cdot \int_D (\nabla Ln \times \nabla \phi) \nabla^2 Ln$, $\int_D \nabla Ln \cdot \nabla [\tilde{g} \partial_2 (Ln - \phi)] = -\int_D \tilde{g} \partial_2 (Ln - \phi) \nabla^2 Ln$, and $\int_D \nabla Ln \cdot \nabla [D(\nabla^2 Ln + |\nabla Ln|^2)] = -\int_D D(\nabla^2 Ln + |\nabla Ln|^2) \nabla^2 Ln$.
- (e) Note that $(\nabla^2 Ln)^2 \geq 0$, $-2\hat{\mathbf{b}} \cdot (\nabla Ln \times \nabla \phi) \nabla^2 Ln \leq |\nabla \phi|^2 + |\hat{\mathbf{b}} \times \nabla Ln|^2 (\nabla^2 Ln)^2 = |\nabla \phi|^2 + |\nabla Ln|^2 (\nabla^2 Ln)^2$, $-2|\nabla Ln|^2 \nabla^2 Ln \leq |\nabla Ln|^4 + (\nabla^2 Ln)^2$, and $2\tilde{g} \partial_2 (Ln - \phi) \nabla^2 Ln \leq [\partial_2 (Ln - \phi)]^2 + (\tilde{g} \nabla^2 Ln)^2 \leq |\nabla (Ln - \phi)|^2 + (\tilde{g} \nabla^2 Ln)^2$.
- (f) Note that $|\nabla (Ln - \phi)|^2 \leq (|\nabla Ln| + |\nabla \phi|)^2 = 2(|\nabla Ln|^2 + |\nabla \phi|^2) - (|\nabla Ln| - |\nabla \phi|)^2 \leq 2(|\nabla Ln|^2 + |\nabla \phi|^2)$.
- (g) Note that $[f + \delta f, h + \delta h] = [f, h] + [f, \delta h] + [\delta f, h] + [\delta f, \delta h]$.
- (h) Note that $f(x_1, x_2, t) = \sum_{n=0}^{\infty} (x_1 \partial_1 + x_2 \partial_2)^n f(0, 0, t) / n!$, $\hat{h}(k_1, k_2, t) = \sum_{m=0}^{\infty} (-1)^m (q_1 \partial_{k_1} + q_2 \partial_{k_2})^m \hat{h}(k_1, k_2, t) / m!$, and $(1/4\pi^2) \iint (q_1 \partial_{k_1} + q_2 \partial_{k_2})^n e^{-i(q_1 x_1 + q_2 x_2)} dq_1 dq_2 = i^n (\partial_1 \partial_{k_1} + \partial_2 \partial_{k_2})^n \delta(x_1) \delta(x_2)$, where Taylor and binomial expansions have been used, and $\delta(x_i)$ is a Dirac delta function.
- (i) Note that $(x_1 \partial_1 + x_2 \partial_2)^n f(0, 0, t) = \sum_{m=1}^n [n! / m! (n - m)!] x_1^m x_2^{n-m} \partial_2^{n-m} f(0, 0, t)$, $(\partial_1 \partial_{k_1} + \partial_2 \partial_{k_2})^n \hat{h}(k_1, k_2, t) = \sum_{m'=1}^n [n! / m'! (n - m')!] \partial_1^{m'} \partial_{k_1}^{n-m'} \partial_2^{n-m'} \hat{h}(k_1, k_2, t)$, and $\iint x_1^m \partial_1^{m'} x_2^{n-m} \partial_2^{n-m'} \delta(x_1) \delta(x_2) dx_1 dx_2 = (-1)^{m'} m'! (n - m')! \iint x_1^{m-m'} x_2^{n-m-n+m'} \delta(x_1) \delta(x_2) dx_1 dx_2 = (-1)^{m'} m'! (n - m')! \delta_{mm'} \delta_{nn'}$, where Taylor and binomial expansions have been used, and $\delta_{nn'}$ is the Kronecker delta symbol.
- (j) Note that the characteristic equation for the system of ODE's $\partial \widehat{\delta Ln} / \partial t = A \widehat{\delta Ln} + B \widehat{\delta \phi}$ and $\partial \widehat{\delta \phi} / \partial t = C \widehat{\delta Ln} + D \widehat{\delta \phi}$ is the eigenvalue equation $(A - \lambda)(D - \lambda) - BC = 0$, whose solutions are $\lambda_{\pm} = (A + D) / 2 \pm \sqrt{(A - D)^2 + 4BC} / 2$, from which the damping/growth rates can be extracted as $\gamma_{\pm} = \text{Re}(\lambda_{\pm})$.
- (k) Note that $\partial_t \tilde{F}_0 \partial_j \nabla^2 \tilde{F}_0 = -k^2 \partial_j \tilde{F}_0 \partial_j \tilde{F}_0$.
- (l) Note that the corresponding characteristic equation is simply $\lambda^3 + k^2 \lambda = 0$.
- (m) Note that the corresponding characteristic equation is now $\lambda^3 - k^2 \lambda = 0$.

¹P. C. Stangeby, *The Plasma Boundary of Magnetic Fusion Devices* (IOP Publishing, Bristol, 2000).

²V. Naulin, *J. Nucl. Mater.* **363–365**, 24 (2007).

³J. Roth, E. Tsironi, A. Loarte, Th. Loarer, G. Counsell, R. Neu, V. Philipps, S. Brezinsek, M. Lehnen, P. Coad, Ch. Grisolia, K. Schmid, K. Krieger, A. Kallenbach, B. Lipschultz, R. Doerner, R. Causey, V. Alimov, W. Shu, O. Ogorodnikova, A. Kirschner, G. Federici, A. Kukushkin, EFDA PWI Task Force, ITER PWI Team, Fusion for Energy, and ITPA SOL/DIV, *J. Nucl. Mater.* **390–391**, 1 (2009).

⁴J. A. Boedo, *J. Nucl. Mater.* **390–391**, 29 (2009).

⁵A. Zeiler, J. F. Drake, and B. Rogers, *Phys. Plasmas* **4**, 2134 (1997).

⁶O. E. Garcia, V. Naulin, A. H. Nielsen, and J. J. Rasmussen, *Phys. Rev. Lett.* **92**, 165003 (2004).

- 612 ⁷B. D. Scott, *Contrib. Plasma Phys.* **46**, 714 (2006).
 613 ⁸P. Ricci, C. Theiler, A. Fasoli, I. Furno, K. Gustafson, D. Iraj, and J.
 614 Loizu, *Phys. Plasmas* **18**, 032109 (2011).
 615 ⁹P. Ricci, F. D. Halpern, S. Jolliet, J. Loizu, A. Masetto, A. Fasoli, I. Furno,
 616 and C. Theiler, *Plasma Phys. Controlled Fusion* **54**, 124047 (2012).
 617 ¹⁰A. Kendl, *Plasma Phys. Controlled Fusion* **57**, 045012 (2015).
 618 ¹¹F. Riva, C. Colin, J. Denis, L. Easy, I. Furno, J. Madsen, F. Militello, V.
 619 Naulin, A. H. Nielsen, J. M. B. Olsen, J. T. Omotani, J. J. Rasmussen, P.
 620 Ricci, E. Serre, P. Tamain, and C. Theiler, *Plasma Phys. Controlled*
 621 *Fusion* **58**, 044005 (2016).
 622 ¹²X. Garbet, L. Laurent, J.-P. Roubin, and A. Samain, *Nucl. Fusion* **31**, 967 (1991).
 623 ¹³Y. Sarazin and Ph. Ghendrih, *Phys. Plasmas* **5**, 4214 (1998).
 624 ¹⁴Ph. Ghendrih, Y. Sarazin, G. Attuel, S. Benkadda, P. Beyer, G. Falchetto,
 625 C. Figarella, X. Garbet, V. Grandgirard, and M. Ottaviani, *Nucl. Fusion*
 626 **43**, 1013 (2003).
 627 ¹⁵N. Bisai, A. Das, S. Deshpande, R. Jha, P. Kaw, A. Sen, and R. Singh,
 628 *Phys. Plasmas* **11**, 4018 (2004).
 629 ¹⁶N. Bisai, A. Das, S. Deshpande, R. Jha, P. Kaw, A. Sen, and R. Singh,
 630 *Phys. Plasmas* **12**, 102515 (2005).
 631 ¹⁷C. F. Figarella, Ph. Ghendrih, Y. Sarazin, G. Attuel, S. Benkadda, P.
 632 Beyer, G. Falchetto, E. Fleurence, X. Garbet, and V. Grandgirard, *J. Nucl.*
 633 *Mater.* **337–339**, 342 (2005).
 634 ¹⁸C. Colin, P. Tamain, P. Ghendrih, F. Schwander, and E. Serre, *Contrib.*
 635 *Plasma Phys.* **54**, 543 (2014).
 636 ¹⁹S. I. Krashennikov, D. A. D'Ippolito, and J. R. Myra, *J. Plasma Phys.* **74**,
 637 679 (2008).
 638 ²⁰I. Furno, B. Labit, M. Podesta, A. Fasoli, S. H. Müller, F. M. Poli, P.
 639 Ricci, C. Theiler, S. Brunner, A. Diallo, and J. Graves, *Phys. Rev. Lett.*
 640 **100**, 055004 (2008).
 641 ²¹K. Bodi, S. I. Krashennikov, and A. I. Smolyakov, *Contrib. Plasma*
 642 *Phys.* **48**, 63 (2008).
 643 ²²C. Theiler, I. Furno, P. Ricci, A. Fasoli, B. Labit, S. H. Müller, and G.
 644 Plyushech, *Phys. Rev. Lett.* **103**, 065001 (2009).
²³O. Izacard, C. Chandre, E. Tassi, and G. Ciraolo, *Phys. Plasmas* **18**, 062105 (2011).
²⁴R. D. Hazeltine, M. Kotschenreuther, and P. J. Morrison, *Phys. Fluids* **28**, 2466 (1985); **29**, 341 (1986).
²⁵R. D. Hazeltine, C. T. Hsu, and P. J. Morrison, *Phys. Fluids* **30**, 3204 (1987).
²⁶C. Silva, I. Nedzelskiy, H. Figueiredo, R. M. O. Galvão, J. A. C. Cabral, and C. A. F. Varandas, *J. Nucl. Mater.* **337–339**, 415 (2005).
²⁷C. Silva, H. Figueiredo, I. Nedzelskiy, B. Gonçalves, and C. A. F. Varandas, *Plasma Phys. Control. Fusion* **48**, 727 (2006).
²⁸R. Vilela Mendes and J. T. Duarte, *J. Math. Phys.* **22**, 1420 (1981).
²⁹P. Beyer, S. Benkadda, G. Fuhr-Chaudier, X. Garbet, Ph. Ghendrih, and Y. Sarazin, *Phys. Rev. Lett.* **94**, 105001 (2005).
³⁰M. Muraglia, O. Agullo, M. Yagi, S. Benkadda, P. Beyer, X. Garbet, S.-I. Itoh, K. Itoh, and A. Sen, *Nucl. Fusion* **49**, 055016 (2009).
³¹M. Muraglia, O. Agullo, S. Benkadda, X. Garbet, P. Beyer, and A. Sen, *Phys. Rev. Lett.* **103**, 145001 (2009).
³²G. Ciraolo, F. Briolle, C. Chandre, E. Floriani, R. Lima, M. Vittot, M. Pettini, C. Figarella, and Ph. Ghendrih, *Phys. Rev. E* **69**, 056213 (2004).
³³O. Izacard, N. Tronko, C. Chandre, G. Ciraolo, M. Vittot, and Ph. Ghendrih, *Plasma Phys. Controlled Fusion* **53**, 125008 (2011).
³⁴Check Equation (10) of Ref. 15.
³⁵Bear in mind that controllability, in the sense of obtaining stable solutions, is favored by maximising the right-hand side (rhs) of (27), and is opposed by minimising its left-hand side (lhs).
³⁶J. P. Freidberg, *Plasma Physics and Fusion Energy* (Cambridge University Press, New York, 2007).
³⁷Check Equation (7) of Ref. 14 and compare it with (26) herein.
³⁸J. T. Duarte and R. Vilela Mendes, *J. Math. Phys.* **24**, 1772 (1983).
³⁹A. Arai and I. Mitoma, *Math. Ann.* **291**, 51 (1991).
⁴⁰H. Liu, Q. Hu, Z. Chen, Q. Yu, L. Zhu, Z. Cheng, G. Zhuang, and Z. Chen, *Nucl. Fusion* **57**, 016003 (2017).